N-Nitrosation of N-Acetyltryptophan probed by IR spectroscopy of the gaseous anion

ARTICLE *in* CHEMICAL PHYSICS LETTERS · NOVEMBER 2013

Impact Factor: 1.9 · DOI: 10.1016/j.cplett.2013.09.063

Chemical Physics Letters xxx (2013) xxx–xxx

Contents lists available at ScienceDirect

Chemical Physics Letters

journal homepage: www.elsevier.com/locate/cplett

N-nitrosation of *N*-acetyltryptophan probed by IR spectroscopy of the gaseous anion

Francesco Lanucara [a,b], Barbara Chiavarino [a], Simonetta Fornarini [a], Maria Elisa Crestoni [a,*]

[a] *Dipartimento di Chimica e Tecnologie del Farmaco, Università di Roma 'La Sapienza', P. le A. Moro 5, I-00185 Roma, Italy*
[b] *Manchester Institute of Biotechnology, Michael Barber Centre for Mass Spectrometry, School of Chemistry, University of Manchester, Manchester M1 7DN, UK*

ARTICLE INFO

Article history:
Received 7 August 2013
In final form 26 September 2013
Available online xxxx

In memoriam Fulvio Cacace

ABSTRACT

A stable N1-nitroso derivative of *N*-acetyltryptophan, $[NANT\text{-}H]^-$, has been assayed by infrared multiple photon dissociation (IRMPD) in the 'fingerprint' range. IRMPD spectra, interpreted by DFT calculations, display features characteristic of the nitrosation motif, which lack in the native *N*-acetyltryptophan anion, $[NAT\text{-}H]^-$. The most stable $[NANT\text{-}H]^-$ isomers, nicely accounting for the experimental features, present the carboxylic group interacting with the amide and benzene ring hydrogens. The side chain is oriented gauche with respect to the indole plane, while the NNO group may adopt either a syn (**1ds**, global minimum) or an anti (**2da**, 2.7 kJ mol^{-1} higher in energy) configuration.

1. Introduction

Since the discovery of the in vivo synthesis of nitric oxide (NO) and its identification as a short-lived molecule acting in signal transduction, the efforts in unveiling its diverse physiological roles and the mechanisms of transport, release and deposit have dramatically increased [1–5]. The binding of NO is primarily directed to the metal center of heme enzymes. However, some regulatory roles of NO, as well as of other reactive nitrogen species (RNS) that form upon aerobic metabolism, are achieved via covalent modifications of biological compounds, such as proteins, nucleic acids, and lipids [6]. In particular, the S-nitrosation of cysteine residues (forming a SNO functionality) has emerged as an ubiquitous, reversible modification that modulates protein function, and ultimately extends the biological activity of NO [7,8]. The reliable assays available for SNO detection has greatly facilitated the identification of target proteins, whose hypo- or hyper S-nitrosation may be related to a wide range of disease states [9,10].

Depending on the cellular redox state, also the nitrogen atom of the indole ring of tryptophan residues can be nitrosated, as present in albumin, melatonin, or in simple *N*-acetyltryptophan. Nitrosation occurs at physiological pH when the primary amine function is N-blocked. The ensuing *N*-nitrosotryptophan derivatives, which share important pharmacological properties with S-nitrosothiols, like vasorelaxation and inhibition of platelet aggregation [11–13], undergo transfer of the *N*-nitroso function to a variety of nucleophiles [14], including water, nucleotides, and thiols [15], thus performing as endogenous nitric oxide carriers. Recently, the development of specific detection protocols [14,16] has opened up the option of reliable identification of *N*-nitrosoproteins in biological samples. However, in order to gain a comprehensive insight into the functions and mechanisms of denitrosation of *N*-nitrosotryptophan derivatives, it is important to explore their inherent bonding and conformational features at a molecular level. Moreover, the effects of environmental factors, such as the presence of solvent or counterions, may be ascertained by working in the gas phase, a low polarity medium where external interferences are absent. In the present letter, the vibrational signature of the *N*-nitroso group and the underlying structural features have been explored in the bare deprotonated *N*-acetyl-N^1-nitrosotryptophan, $[NANT\text{-}H]^-$, a model for the N-indole group in a peptide environment, in parallel with the native molecule, *N*-acetyltryptophan, $[NAT\text{-}H]^-$, by means of infrared multiple photon dissociation (IRMPD) spectroscopy, which has already shown to be able to provide highly diagnostic clues complementing conventional mass spectrometric inferences [17–24]. This sensitive tool, proven to be a powerful tool to investigate the structure of gaseous (bio)molecules, is an 'action' spectroscopy performed by recording the mass-resolved photofragmentation activated by resonant absorption of multiple infrared photons. The coupling of ion trap mass spectrometry with the high fluence of a tunable IR-free electron laser (FEL) allows IRMPD spectroscopy in the highly informative 'fingerprint' region.

Recently, tryptophan molecules and derivatives have been sampled as either (de)protonated, metal tagged or hydrates species by vibrational or electronic spectroscopy [25–31].

The *N*-nitroso feature within the tryptophan skeleton is now probed for the first time by vibrational spectroscopy in the mid-IR range, relying on the coupling of IRMPD spectroscopy with ab initio molecular orbital calculations. These results confirm IRMPD spectroscopy as a powerful tool in affording structural information about species playing relevant biological roles [32–41].

* Corresponding author. Fax: +39 06 4991 3602.
E-mail address: mariaelisa.crestoni@uniroma1.it (M.E. Crestoni).

0009-2614/$ - see front matter © 2013 Elsevier B.V. All rights reserved.
http://dx.doi.org/10.1016/j.cplett.2013.09.063

2. Experimental

2.1. Materials

All reagents were commercial products (Sigma–Aldrich srl Milan, Italy) and were used as received. Deprotonated *N*-acetyl-L-tryptophan, $[NAT\text{-}H]^-$ (*m*/*z* 245), was obtained by electrospray ionization (ESI) by infusing a 5 μM solution of *N*-acetyl-L-tryptophan in water/methanol (3:1). *N*-Acetyl-N^1-nitrosotryptophan, was formed from the reaction of *N*-acetyl-L-tryptophan (2 mM) and $NaNO_2$ or $Na^{15}NO_2$ (2 mM) in 2.0 mL water/methanol (3:1), followed by a dilution to a few μM concentration. Experimental details are reported in the Supplementary Information. ESI-MS analysis showed a prominent species at *m*/*z* 274 assigned to deprotonated *N*-acetyl-N^1-nitrosotryptophan, $[NANT\text{-}H]^-$, with a mass shift of one unit when the nitroso group is labeled with ^{15}N, $[NA^{15}NT\text{-}H]^-$ (*m*/*z* 275).

2.2. IRMPD spectroscopy

IRMPD experiments on the mass-selected ions were performed in the mid-IR range (950–1950 cm^{-1}) employing a modified Paul ion trap mass spectrometer (Esquire 3000+, Bruker Inc.) coupled to the bright and tunable IR radiation of the FEL beamline at CLIO (Centre Laser Infrarouge d'Orsay). Details on this integrated setup have been previously described [42]. The FEL radiation is generated by a 10–50 MeV electron linear accelerator and delivered in 8 μs macropulses (25 Hz), each containing 500 micropulses (few picoseconds long). Typical macropulse energies are 40 mJ. For the present letter, the electron energy was set to 44 MeV with an average laser power evolving from 900 to 650 mW upon increasing wavelength. In the ion trap, ions were mass selected, and accumulated for 5 ms prior to irradiation for 0.2 s. When the IR beam is in resonance with a vibrational transition, several events of photon absorption and intramolecular vibrational redistribution can heat the species to a threshold energy for fragmentation, typically proceeding along the lowest energy pathway. The ensuing IRMPD spectrum is obtained by plotting the photofragmentation yield *R*, defined as $R = -\ln\{I_P/(I_P + \sum I_F)\}$, where I_P and $\sum I_F$ are the intensity of the precursor ion and the sum of the intensities of the fragment ions, respectively, as a function of the laser frequency [18,43].

2.3. Computational details

Hybrid density functional theory (DFT) calculations at the B3LYP/6-311++G** level of theory were performed to obtain the geometries, energetics and linear IR spectra of low-lying structures of $[NAT\text{-}H]^-$ and $[NANT\text{-}H]^-$, using the Spartan 10 software package.

Harmonic vibrational frequencies were obtained for the most stable conformers, comprised within 20 kJ mol^{-1} relative to the global minimum structure. Harmonic frequencies were uniformly scaled by a factor of 0.973 to attain best agreement between computed and observed absorption frequencies [44]. Stick spectra were convoluted with a GAUSSIAN profile of 20 cm^{-1} fwhm (full width at half maximum).

3. Results and discussion

When electrosprayed $[NANT\text{-}H]^-$ ions at *m*/*z* 274 are mass-selected and exposed to resonant IR excitation, fragment ions are observed at (*m*/*z* 244), resulting by homolytic cleavage of NO, and at *m*/*z* 200 and 185, by subsequent loss of CO_2 and $[C_2H_3O_2]$, respectively. The use of $Na^{15}NO_2$ as the nitrosating reagent leads to a mass shift of one unit for the deprotonated species (*m*/*z* 275), which undergoes loss of ^{15}NO when giving the fragment at *m*/*z* 244. The same fragmentation channels observed by IRMPD are also found upon low-energy collision induced dissociation (CID), recently applied to investigate the fragmentation pathways of various *N*-nitroso peptides [45]. The CID experiments have demonstrated the regiospecific formation of the distonic indolyl N-radical cation by NO loss from protonated *N*-nitrosotryptophan. Given the strictly similar process, the photofragment anion at *m*/*z* 244 observed here formally corresponds to a tautomer of *N*-acetyltryptophan radical anion whereby the negative charge is retained by the carboxylic group and the odd electron is on the indole nitrogen. Recently, two isomeric forms of tryptophan radical cation, the distonic N-radical and the π-radical species, were regiospecifically formed and assayed in the gas-phase, suggesting the lack of interconversion between the two isomers [46]. Figure S1 compares example mass spectra recorded upon mass selection and storage of $[NANT\text{-}H]^-$ ions either with (upper trace) or without (bottom trace) irradiation with IR light tuned at 1463 cm^{-1}. The endothermicity for NO cleavage is found equal to 122 kJ mol^{-1} according to B3LYP/6-311++G** calculations and compares well with the homolytic N–NO bond dissociation energy (120 kJ mol^{-1}) for N-nitrosoindole in acetonitrile [47]. This relatively high thermochemical threshold requires the absorption of multiple photons in order to observe an efficient photofragmentation. The experimental IRMPD spectrum of $[NANT\text{-}H]^-$ in the 950–1950 cm^{-1} wavenumber range is presented in Figure 1a (black profile). For comparison purposes, deprotonated *N*-acetyltryptophan, $[NAT\text{-}H]^-$, the parent species lacking the nitrosation feature, has been assayed by IRMPD spectroscopy (Figure 1b). The photofragmentation of $[NAT\text{-}H]^-$ ions at *m*/*z* 245 proceeds by the exclusive loss of CH_2CO, yielding deprotonated tryptophan ions at *m*/*z* 203, as shown in example mass spectra recorded before (lower trace) and after (upper trace) exposure to the FEL IR radiation (Figure 2S). The same fragmentation pattern is observed upon CID at onset collision energy, pointing out that both IRMPD and low-energy CID proceed by a common path, likely involving the fragmentation along the lowest energy pathway.

The two IRMPD spectra of Figure 1 display three similar absorptions. A pronounced band at 1633 cm^{-1}, and two weaker bands at 1452 and 1324 cm^{-1} in the spectrum of $[NAT\text{-}H]^-$ find a counterpart in two prominent absorptions at 1648 and 1463 cm^{-1}, and a weak

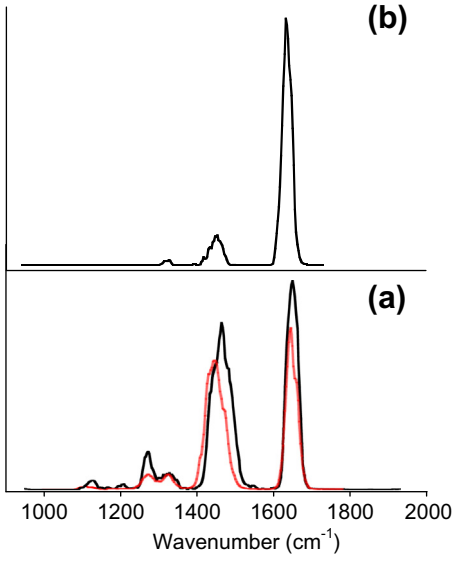

Figure 1. IRMPD spectra of $[NANT\text{-}H]^-$ (a) and $[NAT\text{-}H]^-$ (b) in the 950–1950 cm^{-1} energy range. The red profile in panel (a) shows the IRMPD spectrum of $[NA^{15}NT\text{-}H]^-$. (For interpretation of the references to colour in this figure legend, the reader is referred to the web version of this article.)

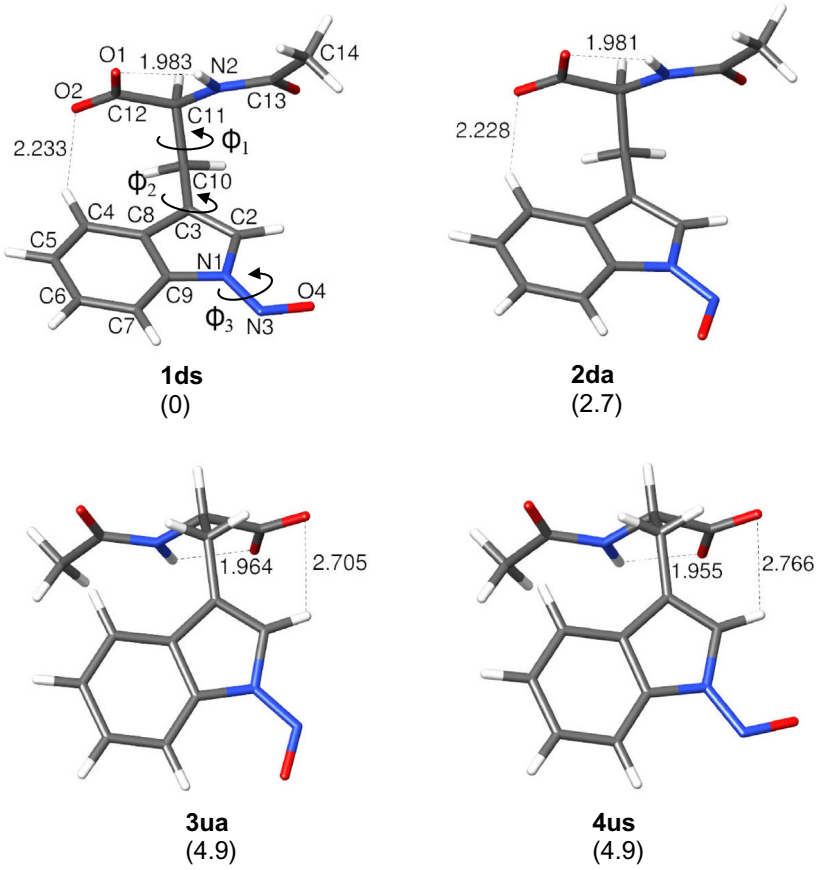

Figure 2. Most stable conformers of deprotonated *N*-acetyl-N^1-nitrosotryptophan $[NANT\text{-}H]^-$ and relative $\Delta H°$ values at 298 K (kJ mol^{-1}) determined at the B3LYP/6-311++G** level of theory. Hydrogen bond distances, marked by dashed lines, are given in Å.

peak at 1325 cm^{-1} in the spectrum of $[NANT\text{-}H]^-$. In addition, the latter species exhibits several weaker bands, the most notable ones at 1020, 1120, 1202, 1273, and 1327 cm^{-1}. To gather direct insights into the IRMPD spectra, which mainly reflect the absorption of the first resonant IR photon, ab initio quantum chemical calculations were performed at the B3LYP/6-311++G** level of theory on the potential candidates, providing optimized geometries, relative energies, and theoretical IR spectra of the sampled ions.

Figure 2 and Figure S3 illustrate ten low-lying structures (the four most stable ones in Figure 2 and the following six in Figure S3) for bare $[NANT\text{-}H]^-$, obtained by stepwise rotation around the C–N and two C–C bonds of the flexible side chain, and all comprised within a 16.8 kJ mol^{-1} energy window. The relevant thermodynamic data, including relative enthalpy and free energy values at 298 K (kJ mol^{-1}), and more complete structural details are provided in the Supplementary Information in Tables S1 and S2, respectively. A common feature is the formal negative charge on the carboxylic group which is engaged in hydrogen bonding with the amide NH group. One may recognize two planes in the molecule, namely the indole ring with the *N*-nitroso group and the plane of the amide linkage in the side chain, which may be oriented yielding either a compact (**1**, **3**, and **9**), or a more extended (**5**, and **7**) conformation. The first structures are gauche isomers with $-90° < \phi_1 < 90°$, while the second ones are trans isomers with $\phi_1 < -90°$. Both sets can be also classified by the orientation of the aromatic ring either upward (denoted with **u**), in structures **3u** and **5u**, or downward (denoted with **d**) in structures **1d**, **7d**, and **9d**, with respect to the side chain, described by negative and positive ϕ_2 values, respectively (Table S2). In all structures, the carboxylic group may be rotated in a way to interact with a hydrogen atom belonging either to pyrrole, in **3u**, and **7d,** or to the benzene ring, in **1d**, and **5u**.

By combining these features with the twofold possibility of either syn (denoted **s**) or anti (denoted **a**) configuration of the *N*-nitroso functionality, described by ϕ_3, couples of low-lying structures rather close in energy result, with the syn isomer in general more favored in free energy than the anti counterpart (Table S1). Easy interconversion of syn-anti isomers of electrosprayed $[NANT\text{-}H]^-$ is not expected according to the sizeable rotational barrier of the N–NO bond (67 ± 4 kJ mol^{-1}) determined by variable-temperature ^{15}N NMR analysis of *N*-nitrosomelatonin, which occurs in mixtures of *Z*-syn and *E*-anti conformers (35:65, respectively) [48]. The most stable structures **1ds**, **2da**, **3ua**, and **4us** (all gauche isomers, clearly favored with respect to trans configurations) show significant parameters, including N–N and N–O bond distances, as well as the N–N–O angle (Table S2) very similar to those observed in other *N*-nitroso compounds [49]. The syn-down isomer **1ds** is found to be the global minimum, with the anti-down isomer **2da**, lying 2.7 (2.8) kJ mol^{-1} higher in enthalphy (free energy), and the syn- and anti-up isomers, **4us**, and **3ua**, almost degenerate, at 4.9 (4.9) and 4.9 (5.1) kJ mol^{-1} in enthalpy (free energy) relative to **1ds**, respectively.

A similar computational analysis has been carried out on $[NANT\text{-}H]^-$, giving the five low-lying conformers (**1d**, **3u**, **5u**, **7d**, and **9d**), all comprised within a 16.8 kJ mol^{-1} energy window, whose geometries are strictly comparable to those of $[NANT\text{-}H]^-$, on the basis of their similar molecular structure (Figure S4). The most stable form, the gauche-up isomer **3u**, lies 3.7 (2.5) kJ mol^{-1} below the enthalpy (free energy) of the trans-down form **7d** (Table S1). Both structures feature a favorable orientation of the carboxylic group

thus enabling stabilizing interactions with both the amide and pyrrole hydrogens. Noteworthily, a change of the preferred orientation of the aminoacid chain is observed when the most stable structures (**1ds** and **2da**) of $[NANT\text{-}H]^-$ are evaluated vs those (**3u** and **7d**) of $[NAT\text{-}H]^-$. One possible explanation may be related to the preferred interaction of the carboxylate with the nearby C–H group which bears the larger amount of positive charge, namely the benzene hydrogens in **1ds**, and **2da**, and the pyrrole hydrogens in **3u**, and **7d**.

The relative entalpies (free energies) of the most stable structures found in both $[NANT\text{-}H]^-$ and $[NAT\text{-}H]^-$ suggest that these species should significantly contribute in a Maxwell–Boltzmann averaged ion population at 298 K.

For comparison purposes, Figure 3 presents the IRMPD spectrum of $[NANT\text{-}H]^-$ along with the calculated IR spectra of the most stable species **1ds** and **2da**, while an exhaustive presentation of linear IR spectra of all calculated structures is provided in Figures. S5 and S6. Owing to the similarity of the IR spectra of the calculated structures, the experimentally observed features are assigned by comparison with the computed vibrational modes of the lowest energy isomers **1ds** and **2da**, which very well account for all the main observed absorptions (Table S3). The dominant band at 1650 cm^{-1} encompasses the amide carbonyl and the antisymmetric carboxylate stretching modes. An envelope of CH_2 scissoring, NH and aromatic CH bend, and NO stretch is responsible for the wide experimental band at 1463 cm^{-1}. Interestingly, the latter mode occurs close by the feature at 1460–1488 cm^{-1} found for deprotonated S-nitrosocysteine, the prototypical compounds for natural S-nitrosothiols [38]. At lower wavenumbers, the feature at 1327 cm^{-1} comprises the symmetric carboxylate stretching, and aromatic CH bending modes, while the adjacent peak at 1273 cm^{-1} is associated to CN and NN stretches. The peaks recorded at 1202, 1120, and 1020 cm^{-1} are assigned to CH_2 wagging, N–N and CN stretches, aromatic CH bend, and aliphatic CC stretch. Interestingly, few distinct, diagnostic bands, calculated at 1198 and 1212 cm^{-1} for **1ds**, and at 1020 cm^{-1} for **2da** denote the presence of both isomers in the thermally averaged sampled ion population.

Further support to the identification of the NO stretching mode has been gathered by assaying the ^{15}NO-labelled ion $[NA^{15}NT\text{-}H]^-$ where an isotope-sensitive behaviour is displayed by the feature at 1463 cm^{-1} in the unlabelled species which is red shifted at 1445 cm^{-1} (Figure 1a, red profile), while the band at 1650 cm^{-1} remains rather unperturbed. The ^{15}N-response of the NO stretching mode, red-shifted from 1490 to 1472 cm^{-1} in the calculated spectrum of **1'ds**, and from 1486 to 1466 cm^{-1} in the case of **2'da** (Figure S7, Table S3), still not resolved from the amide I vibration, provides unambiguous support for the proposed assignment.

Figure 4 and Figure S8 compare the IRMPD spectrum of $[NAT\text{-}H]^-$ with the calculated IR spectra of the most stable species **3u** and **7d**, and with **1d**, **5u**, and **9d**, respectively. It turns out that the linear absorption spectra are very similar. For $[NAT\text{-}H]^-$ the strong contribution of the NO stretching mode in $[NANT\text{-}H]^-$ is

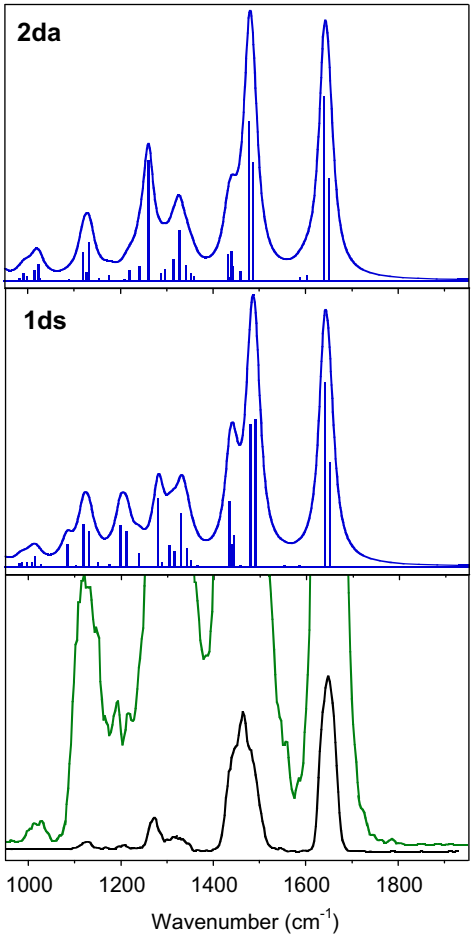

Figure 3. IRMPD spectrum of $[NANT\text{-}H]^-$ (bottom), obtained with full (green) and attenuated by a factor of three (black) laser power, and calculated IR spectra of optimized structures **1ds**, and **2da**. (For interpretation of the references to colour in this figure legend, the reader is referred to the web version of this article.)

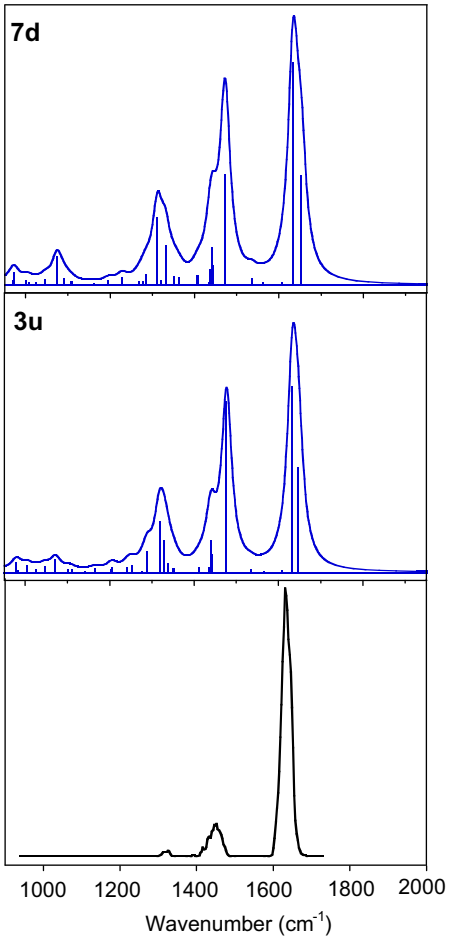

Figure 4. IRMPD spectrum of $[NAT\text{-}H]^-$ (bottom) and calculated IR spectra of optimized structures **3u**, and **7d**.

missing, and only a peak of weak intensity is observed at 1452 cm^{-1}, assigned to CH_2 scissoring and NH bend (Table S4). An additional notable difference emerges below 1300 cm^{-1}, where $[NAT-H]^-$, at variance with $[NANT-H]^-$, presents hardly any vibrational activity. It can be noted that the IRMPD spectrum of $[NAT-H]^-$ show large peak intensity deviation from the calculations at difference with the IRMPD spectrum of $[NANT-H]^-$ species. As evidenced in several IRMPD studies, due to the multiphotonic nature of the IRMPD process, the band intensities do not always match the calculated IR intensities, and small absorptions may be even missing in the experimental spectra. It is conceivable that the actual cross section is not sufficient to promote fragmentation by the IRMPD mechanism. In addition, the band intensity might be reduced in the case of pronounced vibrational anharmonicities.

4. Conclusion

Bare deprotonated *N*-acetyl-N^1-nitrosotryptophan, $[NANT-H]^-$, and the native species, $[NAT-H]^-$, obtained by electrospray ionization, have been investigated by IRMPD spectroscopy in the 950–1950 cm^{-1} spectral range using the FEL CLIO laser coupled with tandem mass spectrometry. The experimental features have been assigned by comparison with IR linear absorption spectra of the lower-lying equilibrium structures calculated at the B3LYP/6-311++G** level. Both the modified and the parent ionic species comprise a population of different conformers at room temperature, whose gaseous conformations and intramolecular interactions have been inferred.

The diagnostic NO stretching mode yields a broad, unresolved band in association with NH bending (so-called amide II band). The assignment is corroborated by the red-shift observed upon ^{15}N-labelling, providing a clear, spectroscopic signature of N-nitrosation at a tryptophan residue, a potential target of (dys)regulated (trans)nitrosation processes.

Acknowledgements

We are grateful to Jean-Michel Ortega, Debora Scuderi, Philippe Maître, Vincent Steinmetz, and the CLIO team. Financial support from the Italian MIUR (Prin Project No. 2009W2W4YF_004), by Università degli Studi di Roma La Sapienza, and by the European Commission through the NEST/ADVENTURE program (EPITOPES, Project No. 15637) is gratefully acknowledged.

Appendix A. Supplementary data

Supplementary data associated with this article can be found, in the online version, at http://dx.doi.org/10.1016/j.cplett.2013.09.063.

References

[1] F. Murad, Angew. Chem., Int. Ed. 38 (1999) 1856.
[2] M.W. Foster, T.J. McMahon, J.S. Stamler, Trends Mol. Med. 9 (2003) 160.
[3] J. McCleverty, Chem. Rev. 104 (2004) 403.
[4] E. Aranda, C. Lopez-Pedrera, J.R. De La Haba-Rodriguez, A. Rodriguez-Ariza, Curr. Mol. Med. 12 (2012) 50.
[5] N. Lehnert, W.R. Scheidt, Inorg. Chem. 49 (2010) 6223.
[6] H. Ohshima, Toxicol. Lett. 140–141 (2003) 99.
[7] P.G. Wang, M. Xian, X. Tang, X. Wu, Z. Wen, T. Cai, A.J. Janczuk, Chem. Rev. 102 (2002) 1091.
[8] M. Benhar, J.S. Stamler, Nat. Cell Biol. 7 (2005) 645.
[9] M.W. Foster, D.T. Hess, J.S. Stamler, Trends Mol. Med. 15 (2009) 391.
[10] G. Hao, S.S. Gross, J. Am. Soc Mass Spectrom. 17 (2006) 1725.
[11] N.S. Bryan, T. Rassaf, R.E. Maloney, C.M. Rodriguez, F. Saijo, J.R. Rodriguez, M. Feelisch, Proc. Natl. Acad. Sci. USA 101 (2004) 4308.
[12] T. Rassaf, N.S. Bryan, M. Kelm, M. Feelish, Free Radical Biol. Med. 33 (2002) 1590.
[13] T. Suzuki, H.F. Mower, M.D. Friesen, I. Gilibert, T. Sawa, H. Ohshima, Free Radical Biol. Med. 37 (2004) 671.
[14] M. Kirsch, H.-G. Korth, Org. Biomol. Chem. 5 (2007) 3889.
[15] K. Sonnenschein, H. de Groot, M. Kirsch, J. Biol. Chem. 279 (2004) 45433.
[16] K. Viles, C. Mathai, F.L. Jourd'heuil, D. Jourd'heuil, Nitric Oxide 28 (2013) 57.
[17] J. Oomens, A.J.A. van Roij, G. Meijer, G. von Helden, Astrophys. J. 542 (2000) 404.
[18] J. Lemaire, P. Boissel, M. Heninger, G. Mauclaire, G. Bellec, H. Mestdagh, A. Simon, et al., Phys. Rev. Lett. 89 (2002) 273002.
[19] J. Oomens, B.G. Sartakov, G. Meijer, G. von Helden, Int. J. Mass Spectrom. 254 (2006) 1.
[20] J.R. Eyler, Mass Spectrom. Rev. 28 (2009) 448.
[21] T.D. Fridgen, Mass Spectrom. Rev. 28 (2009) 586.
[22] N.C. Polfer, Chem. Soc. Rev. 40 (2011) 2211.
[23] N.C. Polfer, J. Oomens, Mass Spectrom. Rev. 28 (2009) 468.
[24] J. Roithova, Chem. Soc. Rev. 41 (2012) 547.
[25] N.C. Polfer, J. Oomens, R.C. Dunbar, Phys. Chem. Chem. Phys. 8 (2006) 2744.
[26] J. Oomens, J.D. Steill, B. Redlich, J. Am. Chem. Soc. 131 (2009) 4310.
[27] A. Lagutschenkov, J. Langer, G. Berden, J. Oomens, O. Dopfer, J. Phys. Chem. A 114 (2010) 13268.
[28] W.K. Mino Jr., K. Gulyuz, D. Wang, C.N. Stedwell, N.C. Polfer, J. Phys. Chem. Lett. 2 (2011) 299.
[29] P. Carcabal, R.T. Kroemer, L.C. Snoek, J.P. Simons, J.M. Bakker, I. Compagnon, G. Meijer, et al., Phys. Chem. Chem. Phys. 6 (2004) 4546.
[30] O.V. Boyarkin, S.R. Mercier, A. Kamariotis, T.R. Rizzo, J. Am. Chem. Soc. 128 (2006) 2816.
[31] A. Fujiwara, N. Noguchi, Y. Yamada, H. Ishikawa, K. Fuke, J. Phys. Chem. A 113 (2009) 8169.
[32] B. Chiavarino, M.E. Crestoni, S. Fornarini, J. Lemaire, P. Maitre, L. MacAleese, J. Am. Chem. Soc. 128 (2006) 1255.
[33] U.J. Lorenz, J. Lemaire, P. Maitre, M.E. Crestoni, S. Fomarini, O. Dopfer, Int. J. Mass Spectrom. 267 (2007) 43.
[34] C. Coletti, N. Re, D. Scuderi, P. Maitre, B. Chiavarino, S. Fornarini, F. Lanucara, et al., Phys. Chem. Chem. Phys. 12 (2010) 13455.
[35] R.K. Sinha, B. Chiavarino, M.E. Crestoni, D. Scuderi, S. Fornarini, Int. J. Mass Spectrom. 308 (2011) 209.
[36] F. Lanucara, B. Chiavarino, M.E. Crestoni, D. Scuderi, R.K. Sinha, P. Maitre, S. Fornarini, Inorg. Chem. 50 (2011) 4445.
[37] M.E. Crestoni, B. Chiavarino, D. Scuderi, A. Di Marzio, S. Fornarini, J. Phys. Chem. B 116 (2012) 8771.
[38] F. Lanucara, B. Chiavarino, M.E. Crestoni, D. Scuderi, K. Sinha, P. Maitre, S. Fornarini, Int. J. Mass Spectrom. 330–332 (2012) 160.
[39] B. Chiavarino, M.E. Crestoni, S. Fornarini, S. Taioli, I. Mancini, P. Tosi, J. Chem. Phys. 137 (2012) 024307.
[40] B. Chiavarino, M.E. Crestoni, S. Fornarini, D. Scuderi, J.Y. Salpin, J. Am. Chem. Soc. 135 (2013) 1445.
[41] F. Lanucara, D. Scuderi, B. Chiavarino, S. Fornarini, P. Maitre, M.E. Crestoni, J. Phys. Chem. Lett. 4 (2013) 2414.
[42] L. Mac Aleese, A. Simon, T.B. McMahon, J.-M. Ortega, D. Scuderi, J. Lemaire, P. Maitre, Int. J. Mass Spectrom. 249/250 (2006) 14.
[43] J.S. Prell, J.T. O'Brien, E.R. Williams, J. Am. Soc. Mass Spectrom. 21 (2010) 800.
[44] M.D. Halls, J. Velkovski, H.B. Schlegel, Theor. Chem. Acc. 105 (2001) 413.
[45] E.R. Knudesn, R.R. Julian, Int. J. Mass Spectrom. 294 (2010) 83.
[46] A. Piatkivskyi, S. Osburn, K. Jaderberg, J. Grzetic, J.D. Steill, J. Oomens, J. Zhao, et al., J. Am. Soc. Mass Spectrom. 24 (2013) 513.
[47] X.-Q. Zhu, J.-Q. He, Q. Li, M. Xian, J. Lu, J.-P. Cheng, J. Org. Chem. 65 (2000) 6729.
[48] A.G. Turjanski, Z. Chaia, R.E. Rosenstein, D.A. Estrin, F. Doctorovich, O. Piro, Acta Crystallogr. C 56 (2000) 682.
[49] A.G. Turjanski, F. Leonik, D.A. Estrin, R.E. Rosenstein, F. Doctorovich, J. Am. Chem. Soc. 122 (2000) 10468.